

EXTREME ROLL MOTION IN WIDE FREQUENCY RANGE DUE TO RAPID DRIFT MOTION

Takako KURODA and Yoshiho IKEDA

Graduate School of Engineering, Osaka Prefecture University

1-1, Gakuen-cho, Sakai, Osaka, Japan

Takako_Kuroda@marine.osakafu-u.ac.jp

SUMMARY

Large amplitude roll motion of a ship without bilge keels in heavy regular beam seas is experimentally investigated, and new nonlinear features of ship motions in high waves are revealed. The model in beam seas is completely free to drift motion, and this leads to change of the encounter frequency. Usually, the drift velocity is much lower than the wave velocity in small beam waves, and this effect can be considered to be negligible. The present experiments, however, show that the drift motion induced by high waves changes the encounter frequency and shifts roll resonance to higher frequency. As the results, large roll motion appears in wide frequency range that is higher than roll natural frequency. In addition, the experiments show that a jump phenomenon of roll, heave and drift velocity, and nonlinear features of heave amplitude appear in high waves.

1. INTRODUCTION

Large amplitude roll motion has been investigated by many researchers over the last forty years. Most of the material contains theoretical studies on the nonlinear features of roll in beam seas, and the many model experiments have been conducted.

The purposes of this study are to investigate new nonlinear features in large amplitudes of ship motions experimentally and to clarify the mechanism of these features. Firstly, the measurements of large amplitude ship motion in heavy beam seas are carried out. The experiments shows that, in high beam seas, large amplitude roll motion occurs not only in the frequency region of the roll resonance but also in the wide frequency region higher than the resonant frequency, and that a kind of jump phenomena of roll motion appears. The cause of these phenomena is that drift motion induced by high waves changes encounter frequency and shifts roll resonance to higher frequency. Roll natural period of the model ship used in the experiments are close to heave natural period. There is quite a possibility that the high roll natural frequency has an influence on the nonlinear features in roll motion in heavy beam seas. Secondly, in order to investigate the relation between roll natural frequency and the shifting of roll resonance to a higher frequency, and to confirm a kind of jump phenomenon of roll motion, additional experiments, in which roll natural frequencies of the model are systematically changed, are carried out. The experiments show that the shifting of roll resonance to higher frequency is induced by increasing drifting velocity due to increasing roll natural frequency. A nonlinear feature of heaving motion is also confirmed near the heave natural frequency. Thirdly, the model ship is knocked to induce jump phenomena during the measurement of ship motions in heavy beam seas. The results show that two types of ship motions could appear with different encounter frequency in the same regular wave. Lastly, to

reveal the reason of the nonlinear features shown in the experiments, nonlinear hydrodynamic characteristics in the motion equations for drifting and roll-heave-sway coupling motion are surveyed.

2. MEASUREMENT OF SHIP MOTIONS IN HEAVY BEAM SEAS

In order to investigate nonlinear ship motions in heavy beam seas, the experiments were conducted in the towing tank (60m in length, 3m in width and 1.4m in depth) of Osaka Prefecture University in Japan.

Under condition where the model is free to sway, drift, roll and heave in regular beam seas, ship motions are measured. The height of a rolling rotation axis is adjusted to the center of gravity of the model. Forward speed is zero, $Fn=0$. The model used in the experiments is a 1/40-scale model of a Japanese training ship “Kagoshima-maru” of Kagoshima University, and its body plan and its principal particulars are shown in Fig. 1 and Table 2. To cause large roll motion, the bilge keels are detached, although the actual ship has wide bilge keels attached at S.S. 3 – S.S. 7. Wave heights of incident waves are changed from 2cm to 8cm (from 0.8m to 3.2m in full scale) systematically to investigate influence of wave height on ship motions. Wave frequencies of incident waves are changed in a range of frequencies $9.0 < \omega_w < 4.5$ rad/s including the roll resonant frequency. The roll natural period of model T_R is 1.06 seconds, and the heave natural period T_Z is 0.90 seconds, which are obtained by free decay tests. The characteristic of this ship is that the roll natural period is close to the heave natural period.

2.1 NONLINEAR FEATURE APPEARED IN ROLL MOTION IN HIGH BEAM WAVES

The results of measured roll amplitudes in beam seas are shown in Fig. 2.

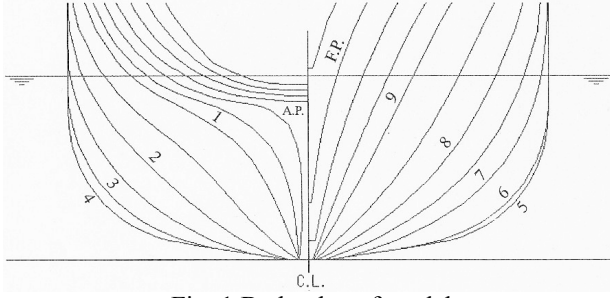


Fig. 1 Body plan of model

Table 1 Principal particulars of model

Items	Model
Scale	1/40
L_{pp} (m)	1.550
B (m)	0.315
d_m (m)	0.120
GM (m)	0.030
KG (m)	0.121
L_{CG} (m)	0.047(aft)
C_b	0.575
ω_z, T_z	6.98, 0.90 _{sec.}
ω_ϕ, T_ϕ	5.93, 1.06 _{sec.}

$\omega_z (=2\pi/T_z)$: heave natural frequency

$\omega_\phi (=2\pi/T_\phi)$: roll natural frequency

The horizontal axis is non-dimensional wave frequency that is defined by dividing wave frequency by the roll natural frequency. The curves in Fig. 2 show the calculated results by Ordinary Strip Method (OSM), in which the roll damping is calculated by Ikeda's Method (Ikeda 1984). In small wave height, the calculated results are in good agreement with the measured ones. However, roll resonance peak significantly shifts to high frequency with increasing wave height. The results demonstrate that large amplitude roll motion occurs not only in the frequency region of the roll resonance but also in the frequency region higher than the resonance frequency in high beam seas. This feature may induce to occur large amplitude roll motion over a wide range of the higher wave frequency where impulsive large wave exciting force due to breaking waves can attack the ship, and causes it to capsize. Moreover, in high waves, at the frequency region of $\omega_w/\omega_\phi \cong 1.30-1.35$, a significant scatters of roll motion appears as shown in Fig. 2. It seems to be a kind of jump phenomenon. It should be noted that the roll amplitude obtained by each measurement in the frequency region is almost steady.

Fig. 3 shows the measured roll amplitudes re-plotted with measured encounter frequencies, which are obtained measured data of ship motions. The response curve of measured results in high waves is smooth, and in comparatively agreement with the calculated ones. In these calculations, period of wave exciting force is regarded to have the encounter period obtained by the

experiment. The shift of the peak frequency of roll motion and the jump phenomena appeared in Fig. 2 cannot be confirmed in this figure.

Fig. 4 shows the relation between wave frequency and encounter frequency with wave height in beam seas. The encounter frequency corresponds to the wave frequency at lower frequency. However, the encounter frequency becomes lower as the wave frequency and wave height becomes higher. It should be noted that the encounter frequency goes down remarkably at the special wave frequency region where the shift of peak frequency of roll clearly appears. This relation between wave frequency and encounter frequency suggests that the drifting velocity rapidly increases with increasing ship motions as incident wave becomes higher.

In order to know variation of the drifting velocity, drifting velocity V_d is calculated by using measured wave frequency and encounter frequency. The drifting velocity V_d is calculated as follows:

$$V_d = \left(1 - \frac{\omega_e}{\omega_w}\right) V_w \quad (1)$$

where wave velocity V_w of incident waves is given by

$$V_w = \frac{g}{\omega_w} \quad (2)$$

where g is acceleration of gravity.

Fig. 5 shows calculated drifting velocity of the ship with encounter frequency. Drifting motion has been analysed by many researchers both theoretically and experimentally. Watanabe (1932) examined that drifting force is the largest at roll resonance, and Tasai (1965) reported that drifting force has maximum values at both roll and heave resonance. The calculated results show that the drifting velocity gradually increase with increasing wave height. In the high waves, the drifting velocity rapidly increases at roll resonance frequency. Moreover, several drifting velocities are obtained at the same wave frequency at the region of wave frequency where the jump phenomenon of roll motion appears ($\omega_e/\omega_\phi = 1.15 \sim 1.2$). These results may demonstrate that the cause of shift of roll resonance peak to higher frequency is that drift motion induced by high waves changes encounter frequency, and the cause of the jump phenomena of roll motion is that several encounter periods exist in the same incident wave.

2.2 INFLUENCE OF ROLL NATURAL FREQUENCY ON NONLINEAR FEATURES

It seems that these nonlinear features mentioned in the previous section are influenced by roll natural period. As said at the beginning, roll natural period of the model ship used in the experiments are close to heave natural

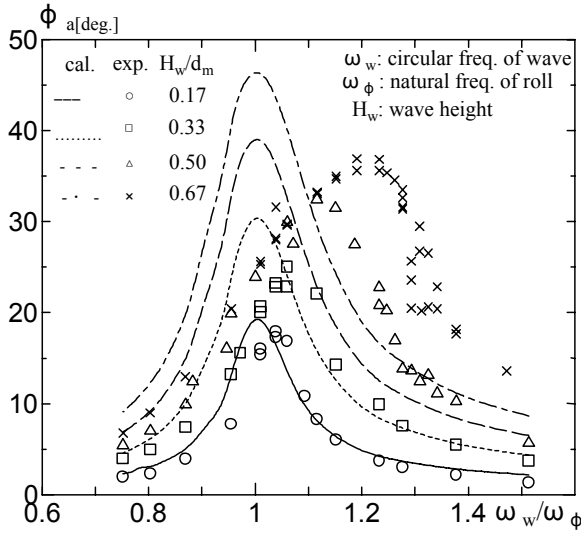


Fig. 2 Measured roll amplitudes in beam seas

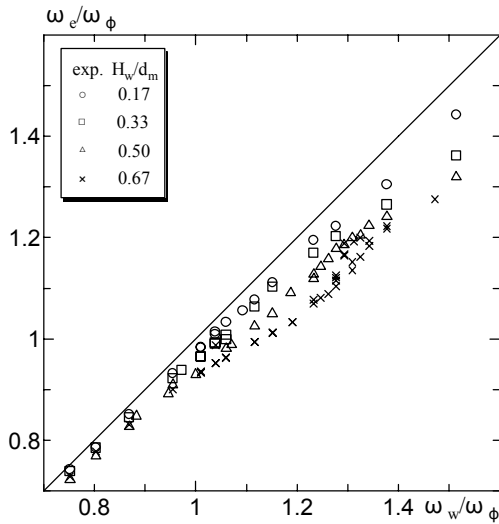


Fig. 4 Relation between wave frequency and encounter frequency in beam seas

period. In order to investigate relation between the roll natural periods and the shift of roll resonance in heavy beam seas, measurements of ship motions with various roll natural periods are conducted. In the experiments, roll natural periods of the model are changed by changing the height of the center of gravity. The model's conditions are shown in Table 2. A standard condition of the ratio of roll to heave natural frequencies is $\omega_\phi/\omega_z = 0.85$. Wave height H_w is 0.08m, and wave periods are changed systematically.

Fig. 6 shows measured roll amplitudes with various roll natural frequencies. In the case of $\omega_\phi/\omega_z = 0.50$, the measured results are in fairly good agreement with the calculated ones. It should be added that measured roll amplitudes rapidly drop in just higher frequency region of roll resonant. As roll natural frequencies become closer to heave natural frequency, roll resonance peak

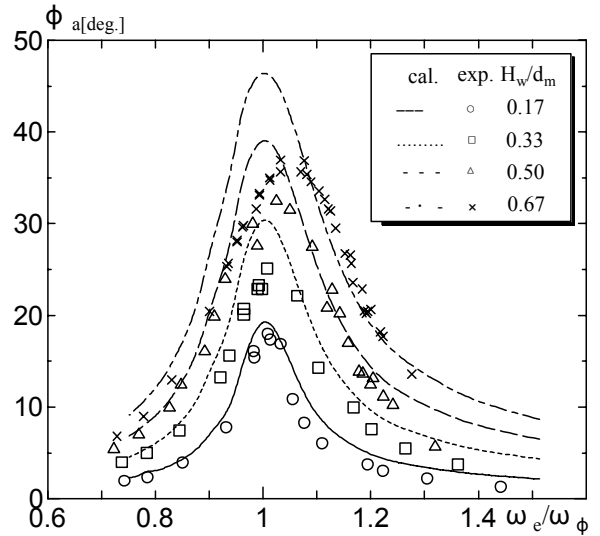


Fig. 3 Re-plotting of measured roll amplitudes with measured encounter frequency

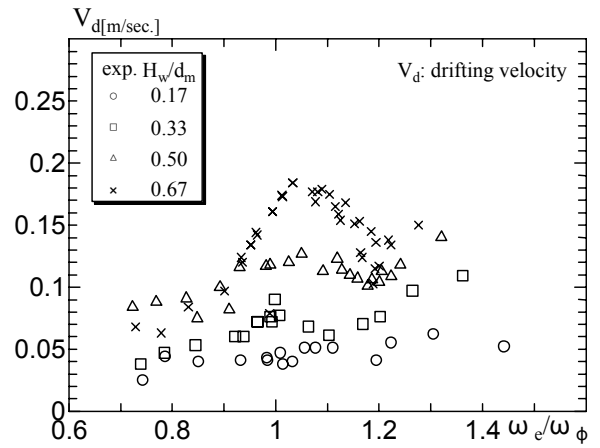


Fig. 5 Calculated drifting velocity from measured encounter frequency

shifts to higher frequency, and the value of roll resonance peak significantly decreases in comparison to calculated ones by OSM. As mentioned in the previous section, the cause of the shift of roll resonance peak to higher frequency is that the drift motion induced by high waves changes the encounter frequency.

Re-plotted results with encounter frequencies are shown in Fig. 7. It should be noted that the experiment was conducted in the frequency region including the resonance frequency (see Fig. 6), but the results for $\omega_\phi/\omega_z = 1.07$ in Fig. 7 have not reached the resonance peak. This fact indicates that effect of drift motion is significant. The frequencies of roll resonance peak are in good agreement with the calculated ones (in this calculation, encounter periods are used as period of wave exciting force). The roll natural frequency becomes higher, calculated results overestimate values of roll resonance peak. These results suggest that, in high

waves, the prediction methods of roll damping and wave exciting force need to be improved.

Fig. 8 shows the relation between wave frequency and encounter frequency for various roll natural frequencies. In the case of $\omega_\phi/\omega_z=0.50$, encounter frequency and wave frequency are closer to each other in the region of low frequency. However, as roll natural frequency becomes closer to heave natural frequency, the encounter frequency becomes lower than wave frequency. This tendency appears as the wave frequency becomes higher.

Fig. 9 shows calculated drifting velocity by Eq. (1). Tasai (1974) reported that drifting velocity increases as encounter frequency becomes higher. In the case of $\omega_\phi/\omega_z=0.50$, the experimental results demonstrate the same characteristic of drifting velocity as he pointed out. It should be noted that drifting velocity at roll resonance increases as roll natural frequency becomes higher. In the present experiments, the incident wave height is constant. Therefore, as roll natural frequency becomes higher, incident wave steepness increases at roll resonance. Tanizawa et al. (2002) reported that drifting velocity is in proportion to the wave steepness. Fig. 10 shows drifting velocity at roll resonant frequency with wave steepness. The results demonstrate that drifting velocity is approximately proportional to wave steepness as he pointed out.

Table 2 Conditions in experiments

ω_ϕ/ω_z	GM (m)
0.50	0.010
0.75	0.023
0.85	0.030
1.00	0.043
1.07	0.048

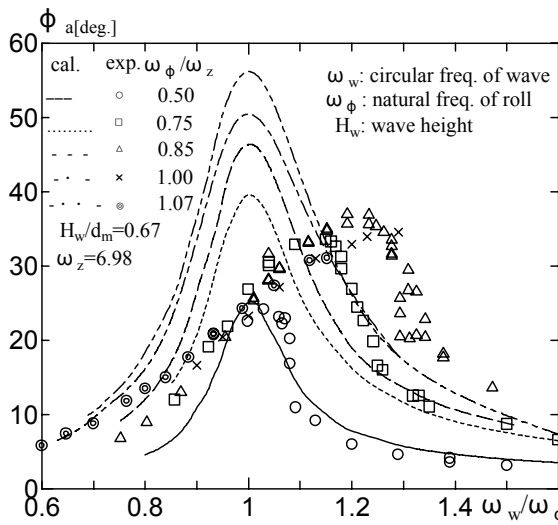


Fig. 6 Measured roll amplitudes vs incident wave frequency

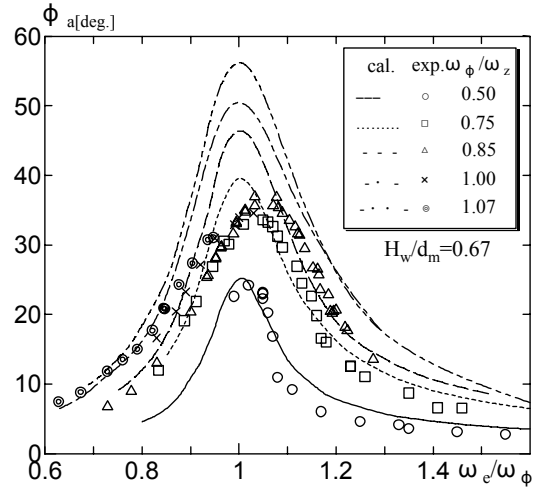


Fig. 7 Measured roll amplitudes with measured encounter frequency

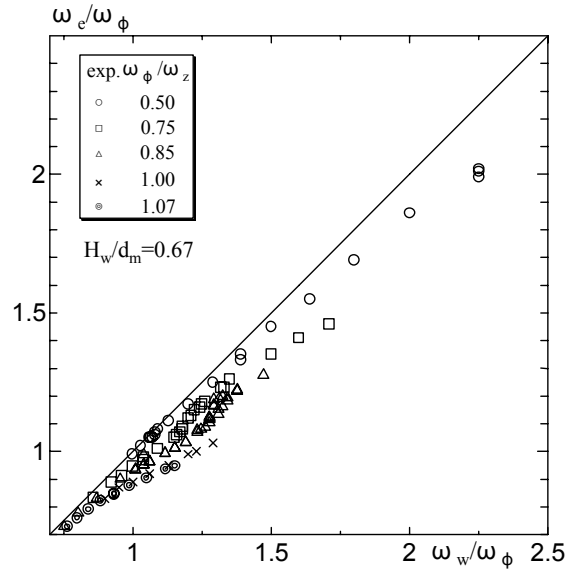


Fig. 8 Relation between incident wave frequency and encounter frequency

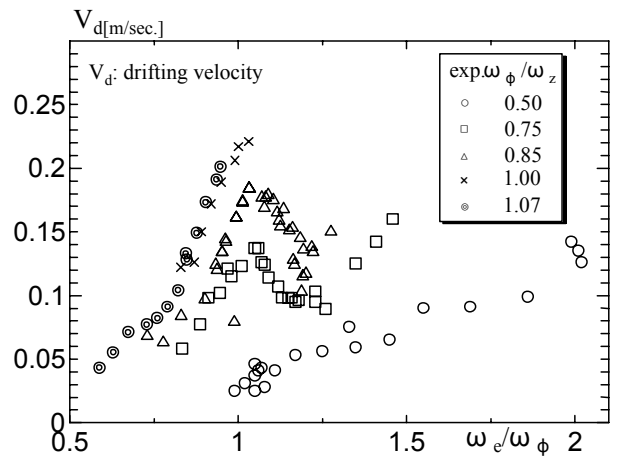


Fig. 9 Calculated drifting velocity from measured encounter frequency

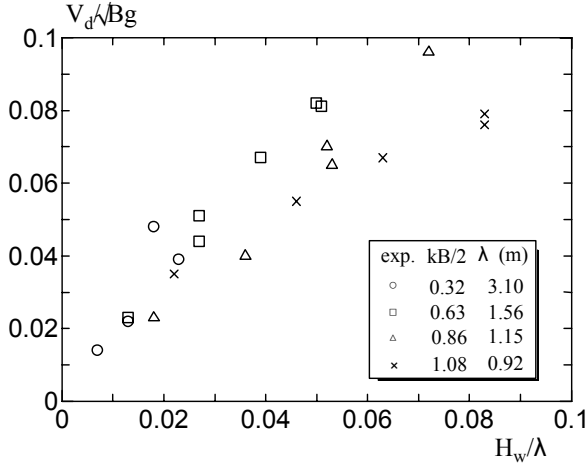


Fig. 10 Drifting velocities at roll resonant frequency with steepness

2.3 NONLINEAR FEATURES IN HEAVE MOTION

In this section, the experimental results of heave motion are explained. Miyake et al. (2002) examined nonlinear heave motion at short wave length in beam and quartering seas, and pointed out that the encounter period region where nonlinear heave motion appears agrees with heave natural period.

Fig. 11 shows measured heave amplitudes for various wave height, and Fig. 12 shows measured heave amplitudes with various of roll natural period in the present study. The strong nonlinear features of heave motion in high waves can be seen. In heavy beam seas, heave amplitudes decrease in the region of heave natural frequency, and this decreasing tendency is remarkably seen as roll natural frequency becomes closer to heave natural frequency. Fig. 13 shows variation of heave amplitude at heave natural frequency. As you can see, heave amplitude decreases by 30% from calculated result by OSM.

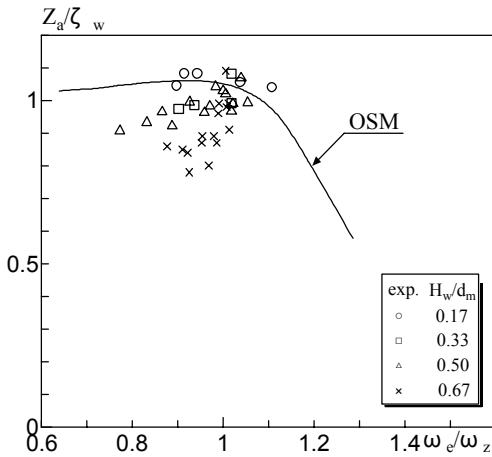


Fig. 11 Measured heave amplitudes with encounter frequency

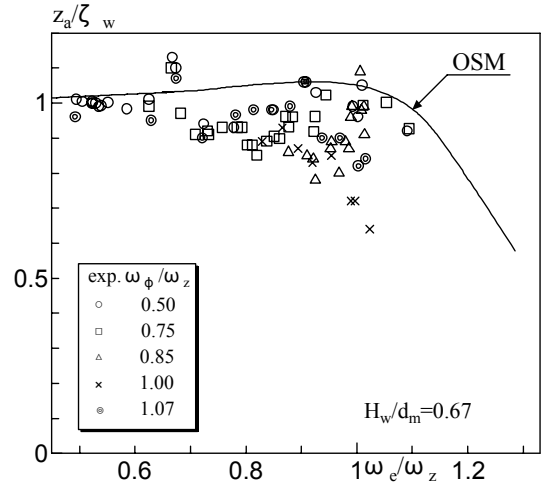


Fig. 12 Measured heave amplitudes with encounter frequency

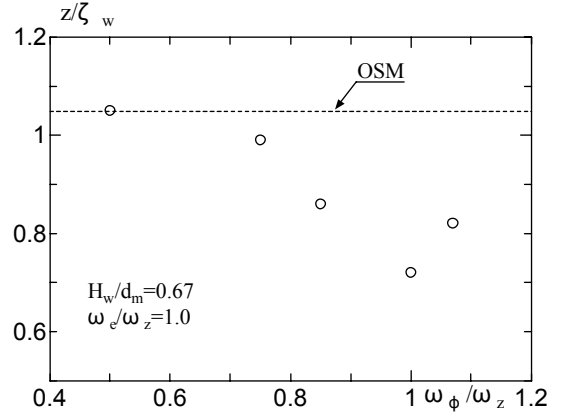


Fig. 13 Deviation of heave amplitude from linear solution at heave resonance frequency

3. CONFIRMATION OF JUMP PHENOMENA IN SUCCESSIVE MEASUREMENTS

As mentioned in previous chapter, a kind of jump phenomenon appears in the experiments. In this chapter, additional experiments to confirm the jump phenomenon are explained.

Experiments of the ship motions in regular beam seas, in which the model is knocked at the side hull, are carried out. Measured time histories of roll and heave motions is displayed in Fig. 14. The existence of two solutions of roll and heave can be seen by knocking the model at a side to sway direction. The experimental condition is \$\omega_\phi/\omega_z = 0.85\$. Wave height is \$H_w = 0.08\text{m}\$ and wave frequency is to be \$\omega_w/\omega_\phi = 1.30\$. As seen in Fig. 14, roll amplitude jumps from small to large. On the other hand, heave amplitude jumps from large to small, and encounter period jumps from short to long by knocking the model. After knocked, each motions and encounter period are almost in steady state.

Two types of motions are observed with different phase angles of heave motion from roll motion. As the encounter period becomes longer, phase angles of heave motion from roll motion approach to zero. Fig. 15 shows phase angles of heave motion from roll motion with various roll natural frequency in $H_w=0.08\text{m}$. The experimental results show some shift to higher frequency from calculated ones by OSM, as encounter frequency becomes higher.

The instantaneous ship attitudes of two types of motion are displayed Fig. 16. These instantaneous attitudes of the ship are obtained on the basis of the measurements of ship motions shown in Fig. 12 and wave profiles. The upper figures show the attitudes in small roll and large heave condition, and the lower ones show the attitude in large roll and small heave condition, respectively. As can be seen in Fig. 16, roll angles at the moment when heave motion stops (the second and fourth figures from left), are significantly different between the upper and lower series. At the moment when heave motion stops, restoring force of heave motion has maximum value. Hence, it is expected that changing water plane area due to large roll angles at the moment may significantly change the restoring force of heave motion. At the moment when velocity of heave motion is fastest (the first, third and fifth figures from left in Fig.16), the relative roll angle to the wave surface is large. At the moment, heave damping is the most dominant component. Then, it is expected that the large relative roll motion may change the heave damping.

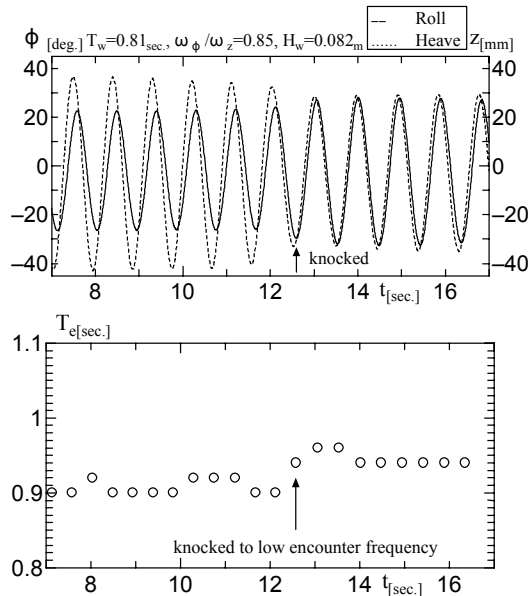


Fig. 14 Experimental evidence for two solutions of roll and heave motions

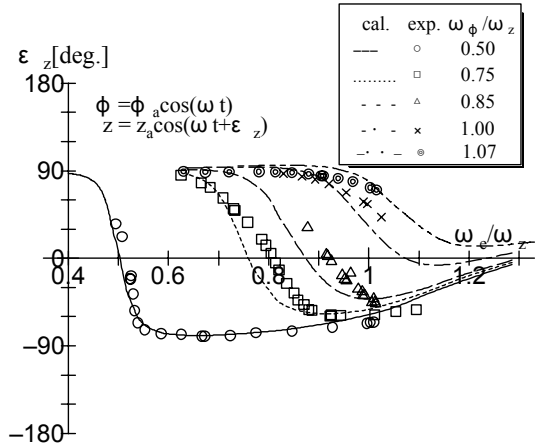


Fig. 15 Phase angles of heave motion from roll motion with encounter frequency in beam seas

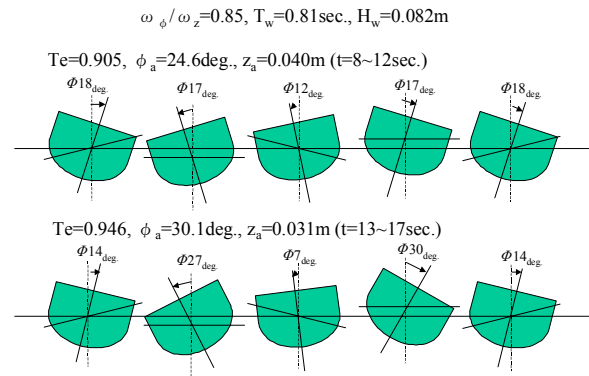


Fig. 16 Instantaneous attitudes of ship in different modes of motion shown during first part ($t=8\sim12\text{sec.}$) and latter part ($t=13\sim17\text{sec.}$) of experimental data shown in Fig.12

4. SURVEY TO FIND CAUSES FOR NONLINEAR FEATURES IN HEAVY BEAM SEAS

The nonlinear ship motions shown in the experiments may be caused by complex interactions between nonlinear hydrodynamic characteristics and coupling motions between steady drift motion, roll, heave, and sway motions. In order to clarify the mechanism of the nonlinear features, nonlinear hydrodynamic forces are experimentally surveyed in this chapter.

4.1 NONLINEARITY OF GZ CURVE

The most popular cause of nonlinear roll motions is non-linearity of roll restoring moment. The GZ-curve of this model, however, has no nonlinear characteristics in the region of measured roll angle up to 38 degrees as shown in Fig. 17. It can be safely said that the non-linearity of roll stability cannot cause the nonlinear roll motions discussed here.

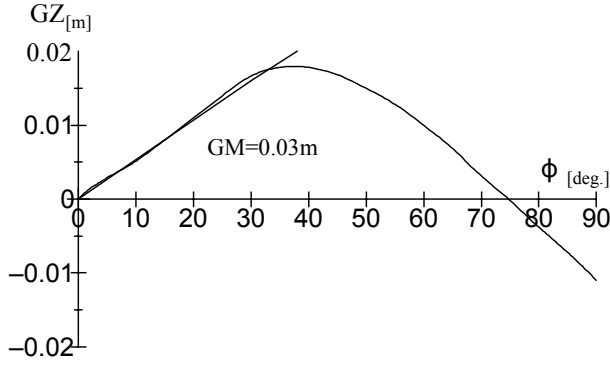


Fig. 17 GZ-curve of the model

4.2 DRIFTING MOTION

As pointed out before, drift motion plays an important role in the nonlinear roll motion. In this section, nonlinear characteristics of wave induced drifting forces and drifting resistance acting on a hull will be investigated.

As well known, drift motion is determined by equilibrium between wave induced drift force F_w and drift resistance F_D . Concerning wave induced drift force, a lot of research has been carried out by Suehiro, Watanabe, Tasai, Maruo (1960) and so on. These studies concluded that the drift force F_w is in proportion to wave height squared. Drift resistance F_D , which is mainly generated by viscous forces, is in proportion to the square of drift velocity V_d . Then, wave induced drift force F_w and drift resistance F_D are expressed as follows:

$$F_w = \frac{1}{2} \rho g C_R^2 \zeta_w^2 \quad (3)$$

$$F_D = \frac{1}{2} \rho S C_D V_d^2 \quad (4)$$

where C_R , S and C_D are coefficient of reflected waves, project area ($=L \times d$), and drift resistance coefficient, respectively. At steady state of drift motion, F_w should coincide with F_D .

C_R is determined by both the diffraction and radiation waves. Fig. 18 shows an example of the calculated drift force F_w acting on the model by a three-dimensional source-distribution method. The result shows that the calculated one varies with roll natural frequency at a higher frequency because roll amplitude at resonance depends on the roll natural frequency. Any causes for the nonlinear roll discussed here cannot be found in the calculated results. Specifically, however, diffraction and radiation wave components depend on the encounter frequency, and must be a function of drifting velocity. Thus, C_R may be a nonlinear function of nonlinear motions in three degrees of freedom and drifting velocity.

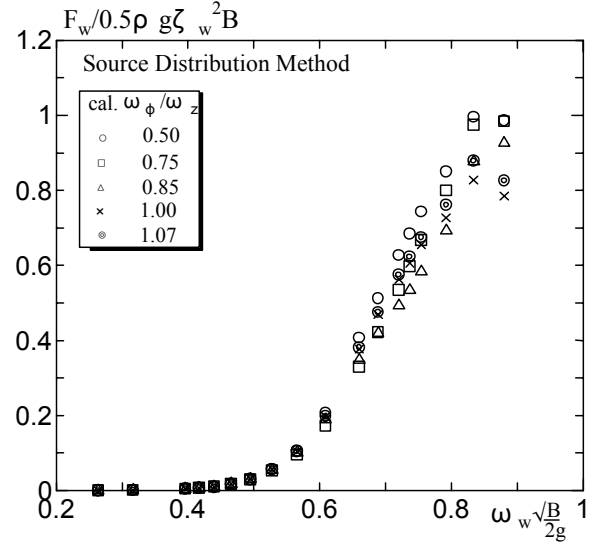


Fig. 18 Calculated drifting force acting on model

Next, resistance acting on a hull in drifting motion will be discussed. When a hull drifts in beam seas, the main component of the resistance force for drift motion is created by vortex shedding due to viscosity. In such a case, the ratio of maximum velocity in sway direction induced by roll motion ' V_R ' to steady drift velocity ' V_d ' is one of important parameters for a vortex shedding pattern as pointed out by Ikeda et al. (1980). Here, V_R can be calculated at the bottom of hull as follows:

$$V_R = d \phi_a \omega_e \quad (5)$$

In the case when V_R/V_d is below unity, as seen in the upper figure in Fig. 19, vortices shed to only weather-side for waves or down-stream side of steady drift motion. On the other hand, in the case of $V_R/V_d > 1$, vortex shedding occurs on both sides, and pressure difference of vortex shedding on each side causes the drift resistance. Fig. 20 shows the ratio of roll velocity V_R to drifting velocity V_d obtained by the experimental data. In the case of $\omega_\phi/\omega_z = 0.50$, the V_R/V_d curve peaks at roll resonance because drift velocity V_d is very small even at roll resonance. In other cases, however, the curves of V_R/V_d are similar each other, and moves above unity. The maximum value is about three. These results suggest that vortices are shed to both sides, and asymmetry vortices generate the drift resistance.

In the region of $V_R/V_d > 1$, the drift resistance may be calculated by using a prediction method of the coupling hydrodynamic forces of roll into sway. Ikeda et al. (1980) proposed a prediction method of the eddy-making component of roll into sway. In the method, the eddy-making component B_{24E} is predicted as follows:

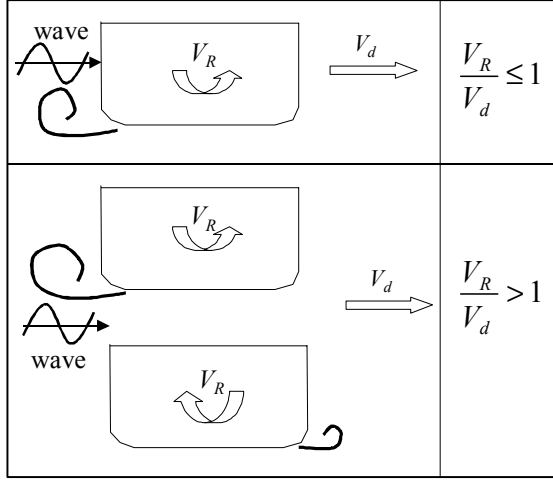


Fig. 19 Schematic views to show mechanism of generation of drifting resistance due to vortex shedding by roll motion

$$\hat{B}_{24E} = \frac{4}{3\pi} \frac{dr_{\max}^2 \left(1 - f_1 \frac{R}{d}\right) \hat{\omega} \phi_0 C_p}{\nabla B} \quad (6)$$

$$f_1 = \frac{1}{2} [1 + \tanh\{20(\sigma - 0.7)\}] \quad (7)$$

where r_{\max} and R are maximum distance from a rotation axis of roll to hull surface and a bilge radius, respectively. An empirical pressure coefficient C_p is expressed as follows:

$$C_p = \frac{3}{4} (0.87e^{-\gamma} - 4e^{-0.817\gamma} + 3) \quad (8)$$

Into the nonlinear force in horizontal direction F_s , which is usually expressed by Eq.(9), Eqs. (6) (7) and (8) are substituted and rearranged.

$$F_s = \frac{3\pi}{8\phi_0\omega} B_{24E} \dot{\phi} |\dot{\phi}| \quad (9)$$

In roll angular velocity, $\dot{\phi}$ in Eq. (9), steady drift velocity should be taken into account. Then, two different F_s , F_s^+ and F_s^- , are calculated by replacing $\dot{\phi}$ by $(V_R + V_d)/r_{\max}$ and $(V_R - V_d)/r_{\max}$. The drift resistance F_D can be obtained by the difference between F_s^+ and F_s^- , and the drift resistance coefficient C_D are represented as follows:

$$F_D = 2\rho d \left(1 - f_1 \frac{R}{d}\right) C_p \left(\frac{V_R}{V_d}\right) V_d^2 \quad (10)$$

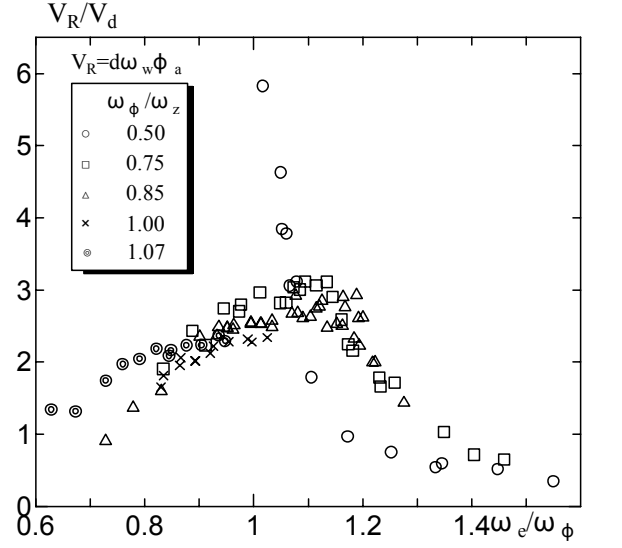


Fig. 20 Ratio of roll induced horizontal velocity at bottom to steady drifting velocity

$$C_D = 2 \left(1 - f_1 \frac{R}{d}\right) C_p \left(\frac{V_R}{V_d}\right) \quad (11)$$

Eq. (10) demonstrates the drift resistance F_D is in proportion to the product of V_R and V_d . Since V_R is a function of roll and V_d depends motions including roll, the drift resistance obtained here must have nonlinear characteristics.

4.3 NONLINEAR HEAVE CHARACTERISTICS DUE TO COUPLING EFFECT OF ROLL INTO HEAVE

In this section, the coupling effect of roll into heave in high waves will be discussed. As pointed out by Tamiya et al. (1969), large roll angle changes water plane area, and this changes the restoring force for heave motion.

Fig. 21 shows variation of the water plane with roll angles for the model, and the dotted line with white circles in Fig. 22 shows variation of water plane area with roll angles. The result shows that the water plane area at roll angle of 33 degrees increased by 12% compared with that at upright position.

Using the water plane area, the effect of its change on heave motion is predicted as follows. The single degree of freedom heave equation expressed by Eq. (12) is used for the calculation.

$$(m_0 + m_{33})\ddot{z} + B_{33}\dot{z} + \rho g A_w z = F_H \quad (12)$$

The calculated results are shown by the broken line with black squares in Fig. 22, and demonstrate that heaving amplitude at maximum roll angle of 33 degrees decrease by 15% comparing with that at upright position. This

fact may suggest that the nonlinear coupling effect between roll and heave can appear in heavy beam seas.

Another possibility of nonlinear features can be expected from the ship motion measurements shown in Fig. 16. At the moment when heave velocity is fastest, the relative roll angle to the wave surface is very large. On this attitude, heave damping, which is in phase with heave velocity, is generated. Then, heave damping may change due to change of submerged hull shape, and there may be some possibility that some nonlinear features are induced in heave motion.

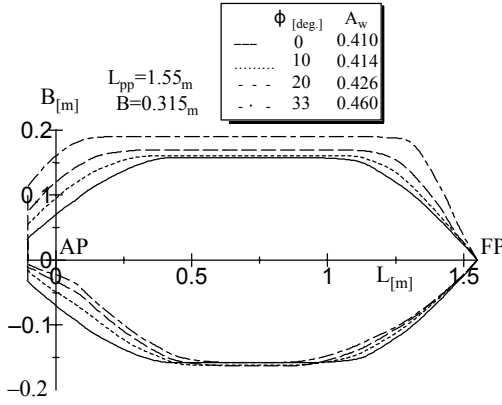


Fig. 21 Variation of water plane with roll angles

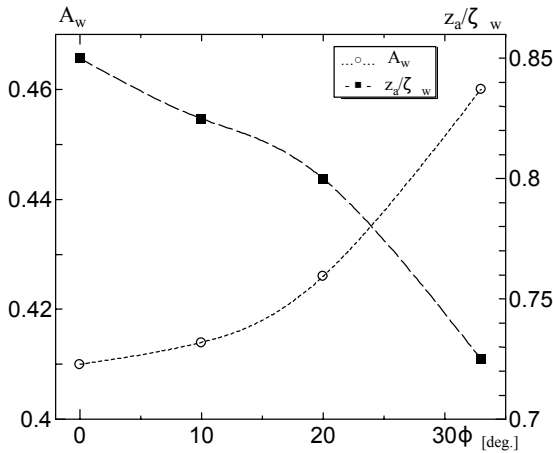


Fig. 22 Variation of water plane area with roll angle and predicted reduction of heave amplitude due to increase of heave restoring force by change of water plane area

4.4 NONLINEAR ROLL CHARACTERISTICS DUE TO COUPLING EFFECT OF HEAVE INTO ROLL

Lastly, nonlinear roll characteristics due to a coupling effect of heave into roll in high waves will be discussed in this section. The importance of the effect was already pointed out by Tamiya et al. (1969).

At heave resonance frequency, relative heave motion to wave surface increases. This means instantaneous draft changes in crest and trough of waves. In the

motions under consideration, since roll resonance frequency is near the heave resonance frequency, roll angles are large at wave crest and trough. Significant interaction between heave and roll motions can then be expected. To confirm this, the roll restoring moment is calculated with various drafts that simulate large relative heave motions in resonance. Fig. 23 shows variation of the GZ-curve with maximum relative heave motion. The result demonstrates that roll restoring moments significantly decrease with decreasing relative heave and slightly increase with increasing relative heave at large roll amplitude. This suggests that large relative heave motions in high waves causes strong nonlinear roll restoring moment.

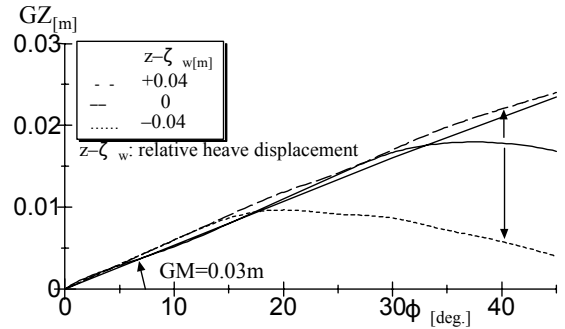


Fig. 23 Variation of roll restoring moment by relative heave motion

5. CONCLUSIONS

Large amplitude roll motions of a ship in heavy regular beam seas is experimentally investigated, and new nonlinear features of ship motions in high waves are revealed. The following conclusions are drawn:

- 1) The experiments shows that, in heavy beam seas, large amplitude roll motion occurs not only in the frequency region of the roll resonance but also in the wide frequency region higher than the resonant frequency, and that a kind of jump phenomena of roll motion appears.
- 2) The cause of the shift of roll resonance peak to higher frequency is that drift motion induced by high waves changes encounter frequency. In the case of jump phenomena of roll motion, several different encounter periods exist for the same incident wave.
- 3) As roll natural frequency becomes closer to heave natural frequency, the roll resonance peak shifts to higher frequency because drifting velocity at roll resonance increases as roll natural frequency becomes higher.
- 4) In high waves, heave amplitudes decrease in the region of heave natural frequency, and this tendency becomes remarkable as roll natural frequency is closer to heave natural frequency.
- 5) Two solutions of roll amplitudes can be observed by knocking the model on its side to sway direction in

heavy beam seas. Roll amplitude jumps from large to small, heave amplitude jumps from small to large, and encounter period jumps from short to long.

- 6) In order to find the causes for the nonlinear features, nonlinear hydrodynamic characteristic in the motion equations for steady drifting motion and oscillating motion are examined. Some nonlinear characteristics can be pointed out.

6. ACKNOWLEDGEMENTS

The authors would like to express thanks to Dr. T. Ikebuti of Kawasaki Heavy Industries (Akashi, Japan), Dr. T. Katayama of Graduate School of Engineering, Osaka Prefecture University, and Prof. R. Shigehiro of Faculty of Fisheries, Kagoshima University, for their helpful advice. This study has been supported by a Grant-in-Aid for Scientific Research of the Ministry of Education, Science, Sports and Culture, Japan (No. 12304065) and Scholarship of Fundamental Research Developing Association for Shipbuilding and Offshore (REDAS).

7. REFERENCES

- Ikedda, Y., 1984. Roll damping. Proceeding of Ship Motions, Wave loads and Propulsive Performance in Seaway, 1st Marine Dynamics Symposium, pp.241-249
- Watanabe, Y., 1932. On the Effective Wave Slope and the Motion of the Center of Gravity of a Ship when Rolling on Waves. *Journal of society of Naval Architects, Japan*, No.49, 1932, pp61-86
- Tasai, F., 1965. Ship Motions in Beam seas. *Journal of West-Japan Society of Naval Architects*, No.30, 1965, pp83-105
- Tasai, F., 1974. On The Drifting Force for Cylinders Floating on Waves, *Journal of Kansai Society of Naval Architects, Japan*, No.152, 1974, pp69-78
- Tanizawa, K., Minami, M. and Imoto, Y., 2002. On the drifting of floating bodies in waves, *Journal of Society of Naval Architects, Japan*, No.190, 2002, pp151-160
- Miyake, R., Zhu, T. and Kagemoto, H., 2002. Experimental Studies on Ship Motions and Wave Loads in Large Waves Using a VLCC Model and a Large-Container Ship Model, *Journal of Society of Naval Architects of Japan*, No.190, 2002, pp75-86
- Maruo, H., 1960. The drift of a Body Floating on Waves, *Journal of Ship Research*, 1960
- Ikedda, Y., Ishikawa, M. and Tanaka, N., 1980, Viscous Effect on Damping Forces of Ship in Sway and Roll Coupling Motion, *Journal of Kansai Society of Naval Architects, Japan*, No.176, 1980, pp31-39
- Tamiya, S. and Watanabe, Y., 1969, Experimental Research on Ship Capsize, *Journal of Society of Naval Architects of Japan*, No.125, 1969, pp89-97